The EuroBiotech Journal
RESEARCH ARTICLE
Medical Biotechnology

Tissue Engineering of 3D-Printed Scaffolds for Breast Cancer Research: A Study on Cell Viability and Adhesion

Belma Nalbant[1,2*], Resit B. Husemoglu[3], Oyku G. Geyik[4], Khayala Rasulova[5], Zeynep Yuce[5], Hasan Havitcioglu[3], Tarkan Unek[6]

Abstract

Objective: Breast cancer remains one of the most prevalent malignancies among women worldwide, underscoring the need for physiologically relevant in vitro models that closely mimic the tumor microenvironment. While two-dimensional (2D) cultures are commonly used, they fall short in replicating in vivo conditions. This study aimed to develop a three-dimensional (3D) breast cancer model using various biomaterial-based scaffolds to evaluate their effects on cell viability, morphology, and adhesion.

Material and Method: MCF-7 breast cancer cells were cultured on five different 3D printed scaffolds composed of PLA, PCL, PET, HIPS, and TPU. Scaffold designs were created using SolidWorks and Slic3r, followed by 3D printing. Cell viability was assessed using the crystal violet assay, and morphological analysis was conducted through scanning electron microscopy (SEM) and confocal microscopy. Statistical analysis was performed using one-way ANOVA.

Results: Among all tested scaffolds, TPU scaffolds exhibited superior performance, significantly enhancing MCF-7 cell viability compared to HIPS, PCL, and PET (***$p \leq 0.001$), and slightly outperforming PLA (ns, $p > 0.05$). SEM analysis revealed enhanced cell spreading and surface attachment on TPU, while HIPS showed minimal interaction. Confocal imaging further confirmed superior nuclear localization and mitochondrial activity on TPU scaffolds, indicating improved metabolic activity and 3D cellular organization.

Conclusion: The findings confirm that TPU scaffolds provide the most supportive microenvironment for MCF-7 cells in 3D culture, offering superior viability, morphology, and cellular interaction. PLA also showed promising results but was slightly less effective than TPU. In contrast, HIPS was the least effective and appears unsuitable as a standalone scaffold material. These results support the use of TPU for physiologically relevant 3D in vitro models of breast cancer for future research and therapeutic applications.

Keywords: 3D cell culture, biomaterials, breast cancer, tissue scaffold; polymers; 3D Printer

[1]Department of Anatomy and Cell Biology, Uniklinik RWTH Aachen, Aachen, Germany
[2]Department of Molecular Medicine, Dokuz Eylul University, Izmir, Türkiye
[3]Department of Biomechanics, Dokuz Eylul University, Izmir, Türkiye
[4]Department of Medical Biology, Istinye University, Istanbul, Türkiye
[5]Department of Medical Biology, Dokuz Eylul University, Izmir, Türkiye
[6]Department of General Surgery, Dokuz Eylul University, Izmir, Türkiye

***Corresponding author:**
Belma Nalbant
Uniklinil RWTH Aachen
Paulwel str. 30, 52074 Aachen, Germany
E-mail: belmanlbnt@gmail.com

DOI: 10.2478/ebtj-2025-0017

Introduction

A Breast cancer stands as the second most prevalent cause of cancer-related mortality among women, making it a pivotal concern within the domain of public health [1]. Initiatives aimed at elucidating the fundamental mechanisms underlying breast cancer are of paramount importance in developing effective treatment modalities. In this context, the initial phase of preclinical investigations often involves in vitro cell culture methodologies [2,3]. The in vitro cell culture technique serves as a fundamental tool for examining various aspects of cancer cell biology, including metabolism, differentiation, proliferation, migration, and mechanical behaviors within biomechanical and biochemical microenvironments. Conventional 2D in vitro cell culture systems, while valuable for studying cellular mechanisms, often lack the necessary realism due to the inherent differences in cellular localization between 2D and 3D environments found in vivo. Consequently, 2D cultures fail to accurately replicate the intricate behaviors of cells at a high resolution. While these systems have their utility, they are insufficient for generating data that mimics in vivo responses, particularly in drug trials. Moreover, their limitations

contribute to increased costs in clinical drug research. The adherence of growing cells impedes their polarization, resulting in disruptions to their interaction with the external environment. This alteration in cellular behavior affects how cells respond to various stimuli and phenomena [4].

3D cultures offer distinct advantages over 2D cultures by more accurately replicating the tumor microenvironment, thereby providing more realistic information [5].

A method developed to address this challenge is 3D cell culture, which enables the creation of environments that facilitate the formation of three-dimensional structures. By allowing cells to grow in a manner akin to in vivo conditions, 3D cell culture systems overcome the limitations of 2D cell cultures. They are applied in various areas such as designing functional tissues for implantation, exploring cancer cell biology, investigating stem cell behaviors, supporting drug discovery efforts, and conducting various cell- or tissue-based analyses [6].

Hence, several approaches within the realm of 3D cell culture offer distinct advantages. One notable method involves the fabrication of scaffolds using biodegradable biopolymers through 3D printing technology [7].

In this study, our objective was to investigate whether breast cancer cells cultured in vitro on 3D scaffolds exhibit superior adhesion and proliferation capabilities compared to the conventional 2D culture model. To achieve this, we fabricated cell scaffolds using a 3D printer and employed various biomaterials, including thermoplastic polyurethane (TPU), polyethylene terephthalate (PET), polylactic acid (PLA), polycaprolactone (PCL), and high-impact polystyrene (HIPS). TPU is becoming increasingly prominent in the field of regenerative medicine, particularly in cardiovascular tissue engineering, due to its biodegradable properties [8].

TPU is commonly preferred for its exceptional properties, including strength, durability, biostability, toughness, low-temperature flexibility, and resistance to abrasion. Moreover, TPU can be used as a composite material in combination with other polymers, enhancing its versatility and broadening its range of applications [9]. PET is extensively utilized in cell culture and medical applications, owing to its key properties such as non-toxicity, biocompatibility, non-carcinogenicity, and biostability. Its linear polymer structure and relatively low melting point further contribute to its adaptability and effectiveness in a wide range of biomedical applications [10]. PLA, a biodegradable synthetic polymer known for its high strength, is widely applied in various fields, including in vitro cell culture, bone tissue engineering, dentistry, and orthopedics [11]. PCL is highly regarded for its excellent compatibility, non-toxic properties, low melting point, cost-effectiveness, and FDA approval, making it a preferred material in a wide range of applications [12].

HIPS polymer is known for its brittle thermoplastic properties, which result in reduced transparency, while also offering advantages such as biodegradability, durability, and stability [13].The breast cancer model used in our study for *in vitro* cell culture was the MCF-7 cell line [14]. This cell line was preferred because of its ability to reflect the properties of a large proportion of all breast cancer types. In addition, extensive research and accumulated knowledge on the characteristics of MCF-7 cells up to date make them a suitable candidate for further analyses [5]

Our previous study on defining MCF-7 cell line growth characteristics on biomaterial tissue scaffolds show that PET and PLA tissue scaffolds were the most supportive in the 3D culture and increase MCF-7 cells by producing an in vivo mimicry microenvironment compared to PCL [15]. In this study, we examined proliferation, the microenvironment in vivo mimic, and the morphology of MCF-7 on other biomaterials.

Material-Methods

Design and Fabrication of Tissue Scaffolds Using 3D Printer

Tissue scaffolds are converted to stl format with the method used before [15]. Tissue scaffolds were fabricated using polycaprolactone (PCL) (Ideaformer, Shenzhen, China), poly(lactic acid) (PLA) (eSun Filament, Shenzhen, China), polyethylene terephthalate (PET) (eSun Filament, Shenzhen, China), high-impact polystyrene (HIPS) (eSun Filament, Shenzhen, China), and thermoplastic polyurethane (TPU) (ColorFabb, Belfeld, Netherlands). The scaffolds were produced using a custom-built 3D printer with a layer thickness of 0.2 mm and a nozzle diameter of 0.3 mm. The nozzle temperatures were set to 210 °C for PLA, 140 °C for PCL, 200 °C for PET, 240 °C for HIPS, and 220 °C for TPU, with a bed temperature maintained at 60 °C for all materials. Both layers were printed with three perimeter lines and a rectilinear infill pattern at a 0–90° orientation, maintaining a flow rate of 100%. The printing speed was standardized at 25 mm/s for all materials.

All scaffolds used in this study were designed as cylindrical structures with a diameter of 4 mm and a height (thickness) of 2.5 mm. The scaffold models were created using SolidWorks 2017 software (Dassault Systèmes, France) and exported as STL files. Slicing and G-code generation for 3D printing were performed using Slic3r version 1.2.9 (Alessandro Ranellucci, Italy) to ensure accurate print resolution and structural consistency across all materials. This standardized design allowed for consistent surface arena and volume in TPU, PCL, PET, PLA, and HIPS scaffolds, enabling reliable comparison of their effects on 3D cell culture.

Determination of Mechanical Characterization of Tissue Scaffolds

The mechanical properties of the scaffolds were evaluated using a universal compression testing machine (Shimadzu Autograph AG-IS 5kN). Compression tests were conducted on five replicates for each scaffold type, including PLA, PCL, PET, HIPS, and TPU. To determine the maximum strength (F max), the scaffolds were compressed to a final thickness of 1 mm at a constant rate of 5 mm/min, with real-time data acquisition performed using Trapezium software.

Culture of MCF-7 Cells onto Tissue Scaffolds

To determine the optimal tissue scaffold for MCF-7 cell culture, cells were seeded onto the scaffolds following standard procedures. Initially, frozen MCF-7 cells were thawed and cultured in complete RPMI-1640 medium (Gibco, Thermo Fisher Scientific, MA, USA; Cat. No: 31870082) supplemented with 10% fetal bovine serum (FBS; Sigma-Aldrich, Cat. No: F7524), 1% insulin (Sigma-Aldrich, Cat. No: I9278), and 1% penicillin-streptomycin (Sigma-Aldrich, Cat. No: P4333) in a T-75 flask. The cells were maintained in a humidified incubator at 37 °C with 5% CO_2.

Prior to cell seeding, tissue scaffolds were sterilized using ethylene oxide to ensure aseptic conditions. The scaffolds were then placed into a 96-well plate, and each well was seeded with 1.5×10^5 cells in complete culture medium. The cell-loaded scaffolds were incubated for 10 days, and the culture medium was refreshed every 72 hours to maintain optimal growth conditions.

Crystal Violet Staining

Cell viability was assessed using crystal violet staining, following the methodology established in our previous study [15]. Once the cells reached confluency in the T-75 flask, the scaffolds were removed from the 96-well plate for staining.

To begin, the scaffolds were washed with phosphate-buffered saline (PBS; Gibco, Thermo Fisher Scientific, MA, USA) to remove any residual culture medium and eliminate non-adherent or dead cells. Adherent cells were fixed and stained using 0.5% crystal violet solution (Sigma-Aldrich, Cat. No: C0775). After staining, scaffolds were allowed to air dry at room temperature. Images of adherent cells were captured using an Olympus CKX41 inverted microscope (Olympus Corporation, Japan) at 10× and 20× magnifications, equipped with a UIS2 digital camera system.

Confocal Microscopy

MitoTracker™ Deep Red FM (MTDR; Molecular Probes, Invitrogen, Thermo Fisher Scientific, Cat. No: M22426) was used to label mitochondria in MCF-7 cells cultured on scaffolds, following the manufacturer's instructions. Cells were incubated with MTDR for 30 minutes at 37 °C, followed by two washes with phosphate-buffered saline (PBS; Gibco, Thermo Fisher Scientific, MA, USA) at room temperature to remove excess dye.

The cells were then fixed with 4% paraformaldehyde (PFA; freshly prepared) for 15 minutes in the dark to preserve cellular structures. After fixation, scaffolds were rinsed again with PBS. Nuclear staining was performed using UltraCruz® Mounting Medium with DAPI (Santa Cruz Biotechnology, Cat. No: sc-24941). Confocal microscopy images were acquired using a Zeiss LSM880 confocal microscope (Carl Zeiss AG, Germany) at 40× magnification. Image processing and 3D reconstruction were performed using ZEN software (Zeiss, Germany)

Scanning Electron Microscopy

Freshly prepared 4% paraformaldehyde (PFA) was used to fix the cells on the scaffolds for 20 minutes at room temperature. After fixation, the samples were dehydrated through a graded ethanol (EtOH) series consisting of 60%, 70%, 80%, and 99% (v/v) for 10 minutes at each concentration, all conducted at room temperature. To facilitate complete drying, the scaffolds were rapidly frozen using liquid nitrogen.

After drying, the samples were coated with a thin layer of gold for 30 seconds using a sputter coater (Quorum Technologies, UK) to enhance surface conductivity. Subsequently, cellular morphology and scaffold surface characteristics were examined using a field emission scanning electron microscope (FE-SEM; ZEISS Sigma 500 VP, Carl Zeiss AG, Germany). High-resolution electron micrographs were obtained at magnifications ranging from 235× to 3174×. Scale bars representing either 10 µm or 100 µm are indicated in each panel accordingly.

Statistical Analysis

A non-parametric one-way ANOVA was employed to assess the differences in cell viability among scaffold groups. Tukey's post-hoc test was utilized to conduct pairwise comparisons among groups to determine statistically significant differences. The results were expressed as mean ± standard deviation. A p-value below 0.05 was considered statistically significant, and statistical analyses were conducted using GraphPad Prism software (version 10.0).

Quantitative image analysis was performed using ImageJ software. Nuclei were measured by DAPI channel thresholding and segmentation. The MTDR signal intensity was measured as the average gray value per image. All quantitative results were presented as mean ± standard deviation. Statistical analyses were conducted using one-way ANOVA, followed by Tukey's post-hoc test (GraphPad Prism 10.0), with a significance threshold established at $p < 0.05$

Results

PLA is the strongest under pressure, whereas TPU is the most flexible

The mean maximum compression strength values for the PLA, PCL, PET, HIPS, and TPU scaffold groups were determined as 820.00 N, 303.03 N, 487.03 N, 488.69 N, and 126.94 N, respectively. Figure 1 presents the average maximum compressive strength values for each tissue scaffold, providing a comparative analysis of their mechanical properties. Additionally, Figure 2 illustrates the flexural curves derived from the force-displacement ratio equation for each biomaterial, highlighting their structural response under mechanical stress. All charts were generated using GraphPad software (GraphPad, San Diego, USA). PLA, and TPU scaffolds. PLA was found to be strongest under pressure, followed by HIPS and PET. PCL and TPU were the least pressure-durable biomaterials.

The compressive strength values of the five scaffold groups—TPU, PCL, PET, HIPS, and PLA—were statistically compared

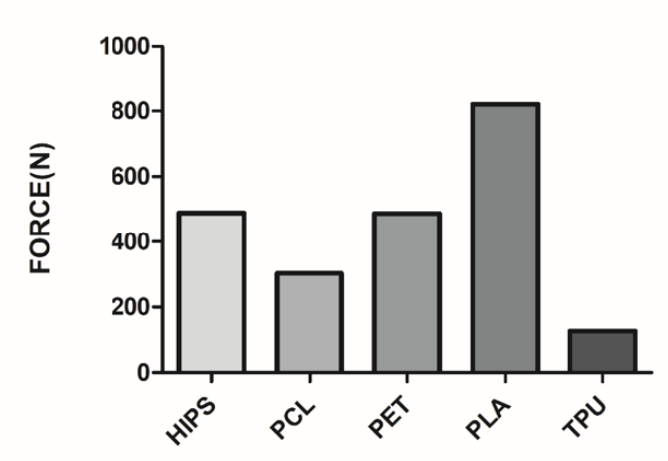

Figure 1. The mean values of maximum compressive strength of HIPS, PCL, PET, PLA, and TPU scaffolds. PLA was found to be strongest under pressure, followed by HIPS and PET. PCL and TPU were the least pressure-durable biomaterials.

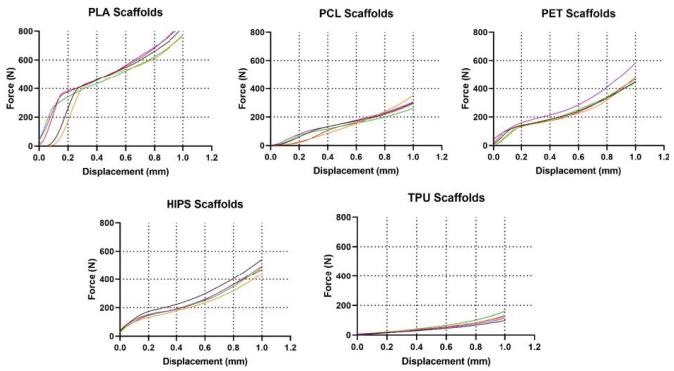

Figure 2. Flexural curves for all biomaterial groups (n=25) were obtained by the force-displacement equation at a displacement rate of 5mm/min. The stress-strain curve showed us its elasticity as strength. TPU has the most flexible structure.

using GraphPad Prism 9 (GraphPad Software, San Diego, CA, USA). Data distribution was first assessed using the Shapiro-Wilk normality test. Since the data did not follow a normal distribution, a non-parametric Kruskal-Wallis test was applied, followed by Dunn's post hoc multiple comparisons test.

Statistical analysis revealed a significant difference in compressive strength among the scaffold groups ($p < 0.001$). PLA scaffolds exhibited the highest compressive strength (mean = 820.00 N), significantly greater than all other groups ($p < 0.0001$ vs. TPU; $p < 0.001$ vs. PCL and PET). HIPS and PET showed intermediate strength values (488.69 N and 487.03 N, respectively), with no statistically significant difference between them ($p > 0.05$). TPU exhibited the lowest compressive strength (mean = 126.94 N), significantly lower than all other materials ($p < 0.0001$ vs. PLA, $p < 0.01$ vs. HIPS and PET). These findings highlight the rigid structural performance of PLA, while demonstrating the soft, flexible nature of TPU. Although TPU exhibited the lowest compressive strength among the tested scaffolds, this result reflects its high elasticity and flexibility rather than structural weakness (Figure 2). In soft tissue engineering applications, such as breast tissue modeling, materials with lower stiffness are often preferred due to their ability to deform under physiological loads without fracturing. The high deformability of TPU allows it to absorb mechanical stress and adapt to complex tissue movements, which is essential in mimicking the mechanical behavior of native soft tissues. Therefore, TPU's low compressive strength can be interpreted as a desirable property for applications requiring elasticity and resilience rather than rigidity.

TPU scaffold represents the most adhesive surface

This experiment was conducted with tissue scaffolds in three technical replicates. Cell-loaded tissue scaffolds were imaged from both the top and bottom, with five images captured per scaffold using a phase-contrast microscope (Olympus CKX41). Cell count analysis performed with ImageJ software revealed that the number of cells adhered to the TPU scaffold was

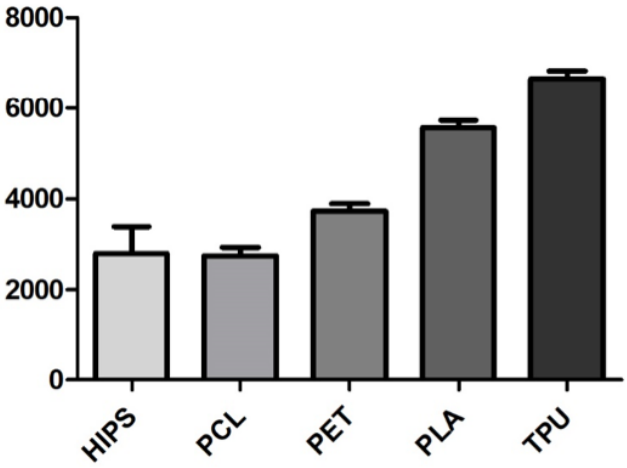

Figure 3. Cell counts on cell scaffolds with ImageJ software (n=5, Bars: SD). Cell density on the surface and layers of the TPU scaffold is better compared to other scaffolds

significantly higher compared to the HIPS, PCL, PLA, and PET scaffolds. The results confirmed that TPU scaffolds supported greater cell adhesion than the other biomaterials tested (Figure 3).

Data analysis was performed using a non-parametric one-way ANOVA test. The statistical results indicated that no significant differences were observed between HIPS

and PCL (ns, $p > 0.05$). Similarly, PCL and PET showed no statistically significant differences (ns, $p > 0.05$). In contrast, PLA and TPU scaffolds demonstrated significantly higher cell viability compared to HIPS, PCL, and PET scaffolds (**$p \leq 0.001$). Moreover, a significant difference was also observed between PLA and PET ($p \leq 0.05$). However, no significant difference was found between PLA and TPU, suggesting that both materials provide comparably favorable environments for supporting MCF-7 cell proliferation. These findings are consistent with the viability trends illustrated in Figure 4.

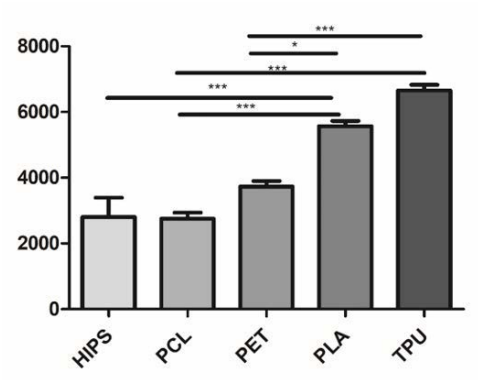

Figure 4. Statistical analyses determined using GraphPad for HIPS, PCL, PLA, PET and TPU scaffolds (n=3, Bars: SD), statistical significance were depicted as; ns: $p > 0.05$, *: $p \leq 0.05$, **: $p \leq 0.01$, ***: $p \leq 0.001$, ****: $p \leq 0.0001$). While TPU and PLA supported cell viability significantly better than HIPS, PCL, or PET, they did not show a significant superiority over each other.

TPU exhibits lower co-localization of red and blue signals than other tissue scaffolds due to higher adhesion of cells to TPU

The MCF-7 cells seeded on the scaffolds, which occupied the architectural textures of the biomaterial matrix in three dimensions, were observed using a confocal microscope (Figure 5). However, confocal microscopy images of the HIPS biomaterial could not be obtained, as the material proved to be brittle and crumbled during the preparation process.

Cells seeded on the biomaterials, other than TPU, displayed co-localization of DAPI and Rhodamine-Phalloidin, indicating a more spheroid-like proliferation pattern. In contrast, the blue and red signals from the cells seeded on the TPU scaffold did not overlap, suggesting that dendritic protrusions were more prevalent with this biomaterial.

This observation highlights TPU's superior supportive properties for cell adhesion and culture, as it facilitated better cellular spreading and extension.

Quantitative evaluation of MCF-7 cell adhesion and mitochondrial activity on various scaffold types. Each group represents n = 3 independent images. Data are presented as mean ± SD. $p < 0.05$ considered significant (One-way ANOVA with Tukey's post-hoc test) (Figure 6,7).

Quantitative analysis of DAPI-stained nuclei revealed that TPU scaffolds supported the highest number of adherent MCF-7 cells, with a mean of approximately 1600 nuclei per field. In contrast, HIPS scaffolds showed the lowest adhesion, with fewer than 1000 nuclei per field. PET, PLA, and PCL scaffolds showed intermediate levels of cell attachment. The differences were statistically significant ($p < 0.0001$, one-way ANOVA), and post-hoc Tukey tests confirmed that TPU

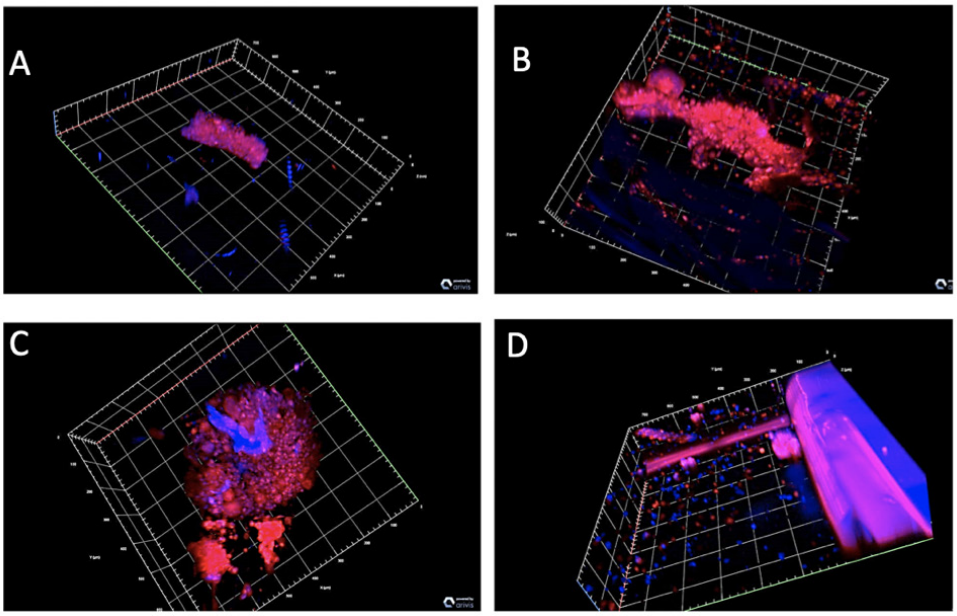

Figure 5. Confocal microscopy images of the MCF-7 cell on tissue scaffolds. A) PCL B) PET C) PLA D) TPU. The blue color is nuclei (DAPI); the red color is MitoTracker Deep Red (MTDR) (Molecular Probes, İnvitrogen, TM). All scale bars indicate 100 µm. TPU exhibits lower co-localization of red and blue signals than other tissue scaffolds due to higher adhesion of the cells to TPU

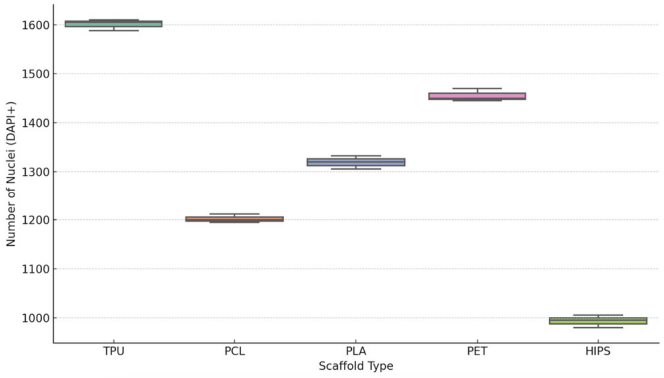

Figure 6. Box and dot plots of DAPI-positive nuclei per field

differed significantly from all other scaffold types ($p < 0.05$). Mean MTDR fluorescence intensity, reflecting mitochondrial activity and cellular metabolic status, was also highest in the TPU group (mean ≈ 43.8 AU), followed by PET, PLA, PCL, and HIPS. Again, statistical analysis showed significant differences across groups ($p < 0.0001$), with TPU being significantly more active metabolically than all others.

These results quantitatively confirm the superior performance of TPU scaffolds in both promoting MCF-7 cell adhesion and maintaining high metabolic activity in 3D culture, validating the qualitative trends observed in the raw confocal

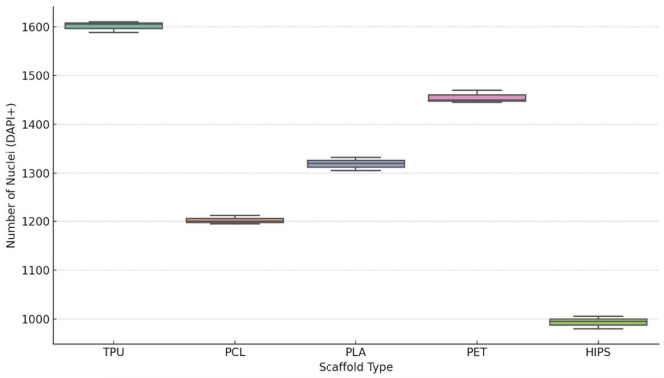

Figure 7. Box and dot plots of MTDR intensity per field

images.

Scanning Electron Microscopy

SEM imaging is a crucial technique for illustrating the inter-layer relationships of cells and their interactions with one another. In this study, it was essential to demonstrate the in vivo mor-

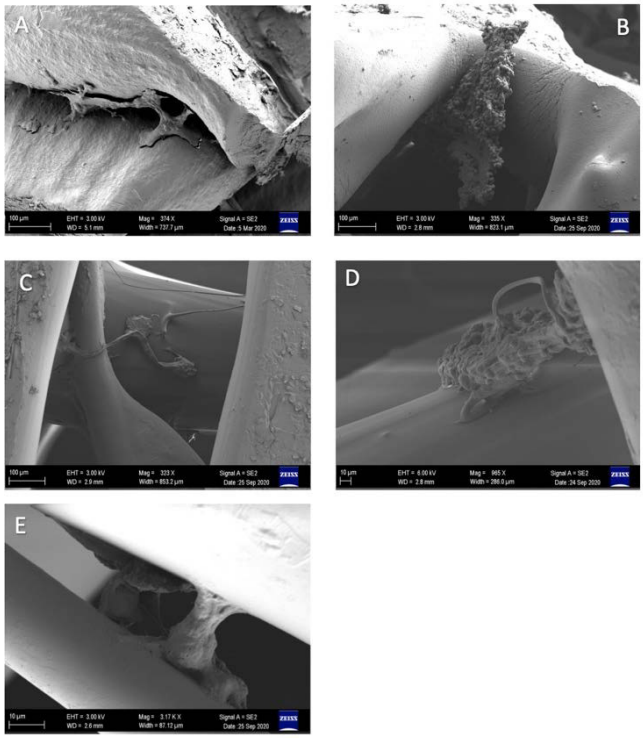

Figure 8. SEM image of the MCF-7 cell on scaffolds. A) HIPS B) PCL C)PET D)PLA E)TPU tissue scaffolds. Cells seeded on HIPS, PET, and TPU tissue scaffolds showed higher extension formations than on PCL and PLA scaffolds. Scale bars indicate 10 µm or 100 µm depending on magnification.

phology and physiology of cells, which were mimicked in the 3D scaffold environment. During image acquisition, both the cells covering the surface and the cell-cell connections between layers were carefully considered. Electron micrographs of the biomaterial scaffold samples with adherent MCF-7 cells were obtained using FE-SEM (Figure 8). The cells on the scaffolds exhibited in vivo-like morphologies, including the formation of extensions either individually or in connection with one another, showcasing the complex cellular interactions and structural behaviours within the scaffold environment.

The interaction of cells between the third and fourth layers serves as a clear indication that the 3D scaffolds can mimic in vivo conditions. This observation suggests that 3D tissue scaffolds hold significant promise for advancing more sophisticated and accurate drug studies, as they provide a more realistic cellular environment compared to traditional 2D models. Such scaffolds can facilitate the development of better therapeutic strategies by offering a more representative platform for evaluating drug efficacy and cellular responses in a controlled, yet biologically relevant, setting.

Discussion

Cancer studies are often conducted using two-dimensional

(2D) in vitro cultures. However, the 2D culture method fails to accurately replicate the morphology and gene expression of cancer cells at the desired resolution and reproducibility. This limitation arises from the fact that 2D cultures do not mimic the complex three-dimensional (3D) architecture of tissues in vivo, leading to a loss of cellular behavior and interactions that are crucial for understanding cancer biology. Consequently, 2D models are insufficient for studying the full complexity of cancer cell dynamics, necessitating the exploration of alternative methods, such as 3D cell cultures, to better simulate the tumor microenvironment [16].

The success of biomaterials in tissue engineering has significantly advanced the field of cell culture. Polymers are particularly favored in cell culture applications due to their key properties, including biocompatibility, cost-effectiveness, and ease of availability. These characteristics make polymers ideal for creating scaffolds that support cell growth and tissue development, offering a versatile and practical solution for a wide range of biological and medical applications. Their adaptability allows for the design of materials that can mimic the natural extracellular matrix, enhancing cellular behavior and facilitating the regeneration of tissues for therapeutic purposes [17].

As the demand for more effective three-dimensional (3D) cell culture systems grows, it is crucial to identify tissue scaffolds that can optimally support the complex architecture of 3D cultures. The selection of appropriate biomaterials is vital for advancing both in vitro and in vivo models. In our previous work, we explored the adhesion properties of MCF-7 cells cultured on 3D printed scaffold models made from various biomaterials, including PLA, PET, and PCL. Our findings indicated that the PLA scaffold outperformed the PCL scaffold in terms of supporting 3D cell culture, aligning with existing studies in the literature. Moreover, similar to other research [15], we observed no significant difference in cell adhesion between PET and PLA scaffolds, underscoring the potential of these materials for effective tissue engineering applications.

In this study, we expanded our understanding of MCF-7 cell adhesion on tissue scaffolds by incorporating HIPS and TPU into our analysis, and by evaluating additional parameters not addressed in our earlier work. Unlike previous studies that focused primarily on adhesion, this investigation also assessed metabolic activity using MitoTracker staining, and cellular localization through confocal microscopy. These added analyses allowed for a more comprehensive comparison of scaffold performance, particularly regarding their ability to support in vivo-like cellular function and morphology.

Compared to PET, TPU, PLA, and PCL scaffolds, the production processes of TPU and HIPS materials were relatively simpler. Due to its rigid and brittle structure, HIPS is not suitable for direct use in cell culture applications and is therefore commonly preferred in composite materials. Previous research by Bougherara et al. demonstrated the effectiveness of HIPS as a composite material, particularly in applications such as bone implants and bone shaping [18]. This study marks the first attempt to use HIPS in cancer cell culture research, and our findings contribute to expanding its potential utility in this field.

Palomeras et al. demonstrated that MCF-7 cell lines cultured on PCL tissue scaffolds serve as effective 3D culture models, supporting adhesion, cell attachment, and the maintenance of appropriate cellular morphology [7]. These results align closely with the findings of our previous study, where we also observed that PCL tissue scaffolds supported MCF-7 cell adhesion, attachment, and morphology in a manner consistent with in vivo conditions [19]. In the present study, improved scaffold design and evaluation using SEM and confocal imaging further validated these observations.

Our current results reaffirm that both PET and PLA scaffolds exhibit moderate support for cell viability and attachment, consistent with our earlier findings [15]. The study by Hassan et al. also reported that PET-based scaffolds promote cell adhesion and proliferation in 3D environments, which was supported by the SEM images obtained in this study [20]. The SEM imaging technique confirmed the establishment of intercellular connections and in vivo-like morphology [20,21]. Confocal microscopy additionally enabled the visualization of nuclear and mitochondrial organization, further verifying scaffold support for 3D cell culture.

However, due to the fragility and rigidity of the HIPS scaffold, it fragmented during preparation, preventing us from obtaining confocal images. SEM images showed mostly rounded, non-spread cells, suggesting poor interaction with the scaffold surface. In contrast, the TPU scaffold—with its fibrous and porous architecture—facilitated higher cell co-localization and metabolic activity, as shown by intense MitoTracker staining and well-distributed nuclei in confocal images. These findings are in agreement with Lis-Bartos et al., who reported superior cell proliferation and intercellular interaction on TPU scaffolds compared to PCL [21].

Our SEM and confocal analyses proved especially informative for characterizing the spatial organization and viability of MCF-7 cells across different scaffolds. In particular, SEM revealed the topographical compatibility of scaffolds with cellular morphology, while confocal imaging provided high-resolution insights into mitochondrial distribution and nuclear positioning. Studies such as Zhang et al. [22] and Yamada et al. [23] have similarly demonstrated that combining SEM and confocal microscopy yields a robust, multidimensional assessment of cell-scaffold interactions, enhancing the reliability of 3D culture evaluations. These integrated imaging approaches help bridge the gap between surface morphology and intracellular behavior, validating scaffold performance in replicating native tissue environments.

Furthermore, the quantitative viability assessment conducted through crystal violet staining and one-way ANOVA revealed that while HIPS, PCL, and PET showed no significant differences among each other, there were marked differences between HIPS and PLA/TPU, as well as between PCL and PLA/TPU. These statistical outcomes emphasize the superior performance of TPU in supporting cell viability. This result is consistent with previous studies showing that scaffold archi-

tecture, porosity, and elasticity significantly influence cellular response in 3D environments [24,25]. Our findings particularly highlight the importance of surface topology and scaffold architecture in improving cellular adhesion and proliferation.

In contrast to the findings of Enayati et al. [8], who found traditional cell culture tools to be more reliable than TPU in in vitro studies, our results indicate that TPU scaffolds provided the best performance in terms of cell adhesion, viability, and morphology among the tissue scaffolds tested on MCF-7 cells. This discrepancy highlights the potential of TPU as a superior scaffold material for enhancing the in vitro culture environment, particularly for applications where cell adhesion and proliferation are critical.

Conclusions

In conclusion, this study compared various cellular scaffolds to determine which best mimics the in vivo microenvironment in terms of cell morphology, adhesion, and viability within a 3D in vitro culture system for breast cancer cells. While all polymers share common properties, such as biocompatibility and biodegradability, they also possess unique structural attributes that lead to varying performance in promoting optimal conditions for the 3D culture of MCF-7 cells. Among the scaffolds tested, the TPU scaffold provided the best results compared to HIPS, PCL, PET, and PLA scaffolds. This study contributes to the growing body of biomaterial literature and will aid in the selection of suitable biomaterials for 3D cell culture applications. Additionally, scaffolds fabricated using 3D printing technology have the potential to significantly enhance drug studies by reflecting the morphology, adhesion, and in vivo-like conditions of cells, offering further integration into research designs for their ability to closely replicate biological systems.

Conflict of Interest Statement

The authors declare that there are no conflicts of interest regarding the publication of this article.

Acknowledgments

This study was partially supported by Defne Ozturk and Melek Ucuncu from Izmir Biomedicine and Genome Center.

Refences

1. Sun Y-S, Zhao Z, Yang Z-N, Xu F, Lu H-J, Zhu Z-Y, et al. Risk Factors and Preventions of Breast Cancer. *Int J Biol Sci.* 2017;13:1387–97.
2. Niu N, Wang L. In vitro human cell line models to predict clinical response to anticancer drugs. *Pharmacogenomics.* 2015;16:273–85.
3. Kitaeva KV, Rutland CS, Rizvanov AA, Solovyeva VV. Cell Culture Based in vitro Test Systems for Anticancer Drug Screening. *Front Bioeng Biotechnol.* 2020;8.
4. Duval K, Grover H, Han L-H, Mou Y, Pegoraro AF, Fredberg J, et al. Modeling Physiological Events in 2D vs. 3D Cell Culture. *Physiology.* 2017;32:266–77.
5. Kapałczyńska M, Kolenda T, Przybyła W, Zajączkowska M, Teresiak A, Filas V, et al. 2D and 3D cell cultures – a comparison of different types of cancer cell cultures. *Arch Med Sci.* 2018;14:910–9.
6. Edmondson R, Broglie JJ, Adcock AF, Yang L. Three-Dimensional Cell Culture Systems and Their Applications in Drug Discovery and Cell-Based Biosensors. *Assay Drug Dev Technol.* 2014;12:207–18.
7. Palomeras S, Rabionet M, Ferrer I, Sarrats A, Garcia-Romeu ML, Puig T, et al. Breast Cancer Stem Cell Culture and Enrichment Using Poly(ε-Caprolactone) Scaffolds. *Molecules.* 2016;21(4):484.
8. Enayati M, Puchhammer S, Iturri J, Grasl C, Kaun C, Baudis S, et al. Assessment of a long-term in vitro model to characterize the mechanical behavior and macrophage-mediated degradation of a novel, degradable, electrospun poly-urethane vascular graft. *J Mech Behav Biomed Mater.* 2020;112:104077.
9. Han D, Chen G, Xiao M, Wang S, Chen S, Peng X, et al. Biodegradable and Toughened Composite of Poly(Propylene Carbonate)/Thermoplastic Polyurethane (PPC/TPU): Effect of Hydrogen Bonding. *Int J Mol Sci.* 2018;19(7):2021.
10. Düzyer Ş. Fabrication of electrospun poly(ethylene terephthalate) scaffolds: characterization and their potential on cell proliferation in vitro. *Textile and Apparel.* 2017;27(3):334–41.
11. Polonio-Alcalá E, Rabionet M, Gallardo X, Angelats D, Ciurana J, Ruiz-Martínez S, et al. PLA Electrospun Scaffolds for Three-Dimensional Triple-Negative Breast Cancer Cell Culture. *Polymers (Basel).* 2019;11(5):916.
12. Feng S, Duan X, Lo P-K, Liu S, Liu X, Chen H, et al. Expansion of breast cancer stem cells with fibrous scaffolds. *Integr Biol.* 2013;5(6):768–77.
13. Mi H-Y, Jing X, Napiwocki BN, Hagerty BS, Chen G, Turng L-S. Biocompatible, degradable thermoplastic polyurethane based on polycaprolactone-block-polytetrahydrofuran-block-polycaprolactone copolymers for soft tissue engineering. *J Mater Chem B.* 2017;5:4137–51.
14. Comşa Ş, Cîmpean AM, Raica M. The story of MCF-7 breast cancer cell line: 40 years of experience in research. *Anticancer Res.* 2015;35(6):3147–54.
15. Geyik OG, Nalbant B, Husemoglu RB, Yuce Z, Unek T, Havitcioglu H. Investigation of surface adhesion of MCF-7 cells in 3D printed PET and PLA tissue scaffold models. *J Biotechnol Biomater.* 2019;6:2161–0487.
16. Gregor A, Filová E, Novák M, Kronek J, Chlup H, Buzgo M, et al. Designing of PLA scaffolds for bone tissue replacement fabricated by ordinary commercial 3D printer. *J Biol Eng.* 2017;11:31.
17. Lynch CR, Kondiah PPD, Choonara YE. Advanced

Strategies for Tissue Engineering in Regenerative Medicine: A Biofabrication and Biopolymer Perspective. *Molecules*. 2021;26(9):2518.
18. Bougherara H, Bureau MN, Yahia L. Bone remodeling in a new biomimetic polymer-composite hip stem. *J Biomed Mater Res A*. 2010;92:164–74.
19. Husemoglu RB, Nalbant B, Geyik ÖG, Ünek T, Yüce Z, Havitçioğlu H. Investigation of surface adhesion abilities of MCF-7 cells on 3D printed PCL and PLA scaffold models. *J Biomater Tissue Eng*. 2019;9(3):217–23.
20. Hassan M, Omar A, Daskalakis E, Hou Y, Huang B, Strashnov I, et al. The potential of polyethylene terephthalate glycol as biomaterial for bone tissue engineering. *Polymers*. 2020;12(5):1032.
21. Lis-Bartos A, Smieszek A, Frańczyk K, Marycz K. Fabrication, characterization, and cytotoxicity of thermoplastic polyurethane/poly(lactic acid) material using human adipose-derived mesenchymal stromal stem cells (hASCs). *Polymers*. 2018;10(10):1073.
22. Zhang J, Liu X, Wang L, Chen Y, Li X. Integration of SEM and confocal microscopy for evaluating cell–scaffold interactions in tissue engineering. *Micron*. 2024;180:103048.
23. Yamada KM, Cukierman E. Modeling tissue morphogenesis and cancer in 3D. *Cell*. 2007;130(4):601–10.
24. Karande TS, Ong JL, Agrawal CM. Diffusion in musculoskeletal tissue engineering scaffolds: design issues related to porosity, permeability, architecture, and nutrient mixing. *Ann Biomed Eng*. 2004;32(12):1728–43.
25. Mishra R, Roux BM, Posner R, Sakiyama-Elbert SE, Dunbar GL. Challenges and prospects of scaffold-based neural tissue engineering. *Biomed Mater*. 2019;14(4):042001.